Coir Fibre and Rope Reinforced Concrete Beam Under Dynamic Loading

Majid Ali[1] and Nawawi Chouw[2]

[1] Corresponding Author, PhD Student; [2]Associate Professor. Department of Civil and Environmental Engineering, the University of Auckland, New Zealand.
Email: [1]mali078@aucklanduni.ac.nz; [2]n.chouw@auckland.ac.nz

Abstract

In order to acquire knowledge for designing low-cost but safe housing in earthquake prone regions, the basic dynamic properties of coconut fibre reinforced concrete (CFRC) structural members is investigated. The outcome of this research will be used in the analysis of CFRC buildings under earthquake loading in the future. Natural coir fibres having a length of 7.5 cm and a fibre content of 3 % by weight of cement are used to prepare CFRC beams. Coconut rope having a diameter of 1cm and tensile strength of 7.8 MPa is added as the main reinforcement. Compressive strength, splitting tensile strength, modulus of elasticity and modulus of rupture for CFRC are investigated. The dynamic behavior and load carrying capacity of CFRC beams as structural members without and with coconut rope are discussed.

Keywords: Coir fibres, coir rope, dynamic loading, natural frequency, damping coefficient

1. INTRODUCTION

Conventional reinforced concrete uses steel rebars. However, steel reinforcement is still expensive for many people who want to build earthquake resistant houses. To overcome the difficulty, an economical but safe constructional material is needed. Natural fibres can be one possible material, as they are cheap and locally available in many countries. In this work, rope made of coir fibre is used as replacement to steel rebars in coir fibre reinforced concrete (CFRC) beams.

Ghavami (2005) and Kankam et al. (1988) tested bamboo as main reinforcement in concrete. However, both researchers considered only static load and they reported satisfactory performance of bamboo reinforced concrete for bearing static load. Li et al. (2007) studied fibre volume fraction and fibre surface treatment with a wetting agent for coir mesh reinforced mortar using nonwoven coir mesh matting. They performed a four-point bending test on a slab specimen. They concluded that cementitious composites, reinforced by three layers of coir mesh (with a low fibre content of 1.8%) resulted in a 40% improvement in the maximum flexural stress, were 25 times stronger in flexural toughness, and about 20 times higher in flexural ductility. Sivaraja and Kandasamy (2008) determined the ductility and energy absorption for concrete composites reinforced with local materials (coir, rice husk and sugarcane). It was found that no crushing and spilling of concrete occurred during the failure. Zheng et al. (2008) and Yan et al. (2000) determined the dynamic properties of concrete composites having scrap tires and polyolefin fibres, respectively. Zheng found that damping ratios of grinded and crushed rubberized concrete (45% by volume of aggregate replaced with rubber) could reach as high as 75% and 144%, respectively, as compared to plain concrete. Yan found that an increase in damping was always accompanied by a decrease in response frequencies for studied fibre reinforced concrete composites.

2 EXPERIMENTAL PROCEDURE

2.1 RAW MATERIALS

Ordinary Portland cement, locally available sand, aggregates, potable water and imported brown coir fibres were used for preparation of plain concrete (PC) and CFRC beams. The maximum size of aggregates was 12mm (passing through sieve 12mm and retained at sieve 10mm). The diameter and tensile strength of coir rope was 1 cm and 7.8 MPa, respectively.

2.2 PREPARATION OF COIR FIBRES

Since fibres were in hydraulic compressed form, preparation of fibres into the required length was a time consuming and laborious task. Different approaches were tried to get fibres into the required length quickly without much success. Finally, coir fibres were loosed and soaked in water for 30 minutes to soften the fibres and to remove coir dust. Fibres were then straightened manually and combed with a steel comb. Wet long fibres were put in an oven where approximately 70-80% moisture was removed; and then fibres were dried in the open air. Fibres were again combed and cut into the required length of 7.5 cm with a guillotine.

Figure 1: Concrete mixer

2.3 MIX DESIGN AND CASTING PROCEDURE

For the plain concrete, the mix design ratio for cement, sand and aggregates was 1, 2 and 2, respectively with a water cement ratio of 0.48. The mix design for coir fibre reinforced concrete was the same as that of the plain concrete except that (1) the water cement ratio was 0.56 because of the addition of fibre to make CFRC workable and (2) 7.5 cm long coir fibres of 3% by weight of cement were added and the same amount (weight) of aggregates were deducted from the total weight of aggregates. All materials were taken by weight of cement.

Figure 2: CFRC mixing technology

The pan type concrete mixer, shown in Figure 1, was used in preparing concrete. All materials were put in the mixer pan along with the water, and the mixer was rotated for three minutes. The slump test was 50mm. For preparing CFRC, a layer of coir fibres was spread in the pan, followed by spreading of aggregates, sand and cement. The first layer of fibres was hidden under the dry concrete materials with the help of a spade. Then, another layer of coir fibres followed by layers of aggregates, sand and cement were spread. Figure 2 shows the second layer of fibres over the dry concrete materials. This process is repeated until the rest materials

Figure 3: CFRC beam with rope

were put into the mixer pan. Approximately, three quarters of the water (according to a water cement ratio of 0.48 which was the same as that of plain concrete) was added, and the mixer was rotated for two minutes. Then the remaining water was added and the mixer was again rotated for two minutes. The CFRC was not workable at this stage, so more water was added twice with an increment of 0.04 water cement ratio to make the CFRC workable. Finally, the mixer was rotated for three minutes to get mix the CFRC well. A slump test for the CFRC was also performed before pouring it into moulds. This test was performed in the same manner as performed for that of plain concrete. The slump test for CFRC was 12mm, but the CFRC was workable using a new pouring technique. It may be noted that more water could not be added to avoid bleeding. CFRC was poured into the moulds and the moulds were lifted up to a height of approximately 200 – 300 mm and then dropped to the floor for self compaction of the fibre concrete and to remove air voids from the CFRC. Figure 3 shows a partially filled CFRC beam with rope. A clear concrete cover below the rope was ensured. It may be noted that the rope was pre-tensioned so that there was no sagging while pouring the CFRC, and knots were provided at both ends just to provide anchorage. All specimens were cured for 28 days before testing.

2.4 SPECIMENS

Cylinders 100mm in diameter and 200mm in height, and small beams 100mm wide, 100mm deep and 500mm long, respectively were prepared for PC and CFRC. Long beams 100mm wide, 100mm deep and 915mm long, were prepared only for the CFRC, because such long beams for PC could break during handling. A set of three samples for each specimen and concrete type (PC and CFRC) were produced. A total of 12 cylinders (6 with PC and 6 with CFRC), 6 small beams (3 with PC and 3 with CFRC) and 4 long beams (3 with CFRC having no rope and 1 with CFRC having coconut rope) were prepared. Labels OO and C3 were used for PC and CFRC, respectively. A, B and C (also D, E and F for cylinders splitting tensile strength testing) along with labels depicted the mark of the sample for each specimen. C3R is the mark for the CFRC beam with rope. All specimens were white washed before testing for clear identification of cracks.

2.5 TESTING PROCEDURE

2.5.1 CYLINDER TESTS

All cylinders were tested in a compression testing machine to determine compressive strength (σ), corresponding strain (ε), modulus of elasticity (MOE) and splitting tensile strength (STS). Each cylinder was capped with plaster of Paris for uniform distribution of load before testing of the MOE. Figures 4(a) and 4(b) show MOE and STS test set ups, respectively.

(a) MOE testing **(b) STS testing**

Figure 4: Cylinder testing

2.5.2 SMALL BEAM TESTS

All small beams were tested in a universal testing machine of capacity 100 kN using 4-point loads to obtain the modulus of rupture (MOR), corresponding deflection (Δ) and cracking load (P_{Crack}). Cracking load is the load taken by fibres after the first visible crack is produced.

2.5.3 LONG BEAM TESTS

Figure 5: Experimental set up for dynamic testing

The experimental set up for testing of long beams is shown in Figure 5. A small impact load ($P_{Max\text{-}impact}$) is applied three times within 20 seconds at midspan of the beam with the help of a calibrated hammer. The response is recorded by accelerometers. Then the same beam is put under a static load ($P_{Max\text{-}static}$) of 1kN in the universal testing machine. Deflection is noted using a LVDT. Again, a small impact load is applied three times and the response is recorded. Note that the impact load is applied three times to take the average of resulting three values of a particular dynamic property. This procedure is repeated until failure of the beam. The load before producing the first crack is taken as the reference for the just before crack stage. Dynamic properties of the beams without and with coconut rope are investigated for the four stages; (i) uncracked beam, (ii) just before cracking, (iii) cracked beam and (iv) after cracks occurred following four cycles of static load. Each cycle consists of applying a static load on the cracked beam up to a certain deflection and then releasing the load for measuring its dynamic properties.

3. TEST RESULTS AND ANALYSIS

3.1 STATIC PROPERTIES

Static properties of plain concrete (PC) and coir fibre reinforced concrete (CFRC) are presented in Table 1. All values are average of three readings. There is a slight decrease in compressive strength (σ) and an increase in corresponding strain (ε) and splitting tensile strength (STS) of CFRC as compared to that of PC. The modulus of elasticity is calculated as the ratio of stress change to strain change in the elastic range. Stress-strain curves for MOE and STS are shown in Figures 6 and 7, respectively. Stress-strain relationship for each sample in Figure 6 shows the average of readings taken by two LVDTs (linear variable differential transformers) attached to the specimens (as shown in Figure 4a).

Table 1: Static properties of plain and coir fibre reinforced concrete

Sample	Cylinder testing				Small beam testing			Density (kg/m^3)
	σ (MPa)	ε (%)	MOE (GPa)	STS (MPa)	MOR (MPa)	Δ (mm)	P_{CRACK} (kN)	
PC	35.5	0.175	23.2	3.82	4.71	0.64	-	2277
CFRC	32.6	0.223	21.1	4.17	5.01	0.69	1.08	2257

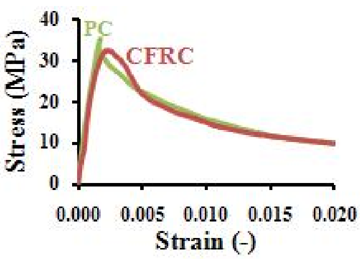

Figure 6: Stress-strain curves for MOE

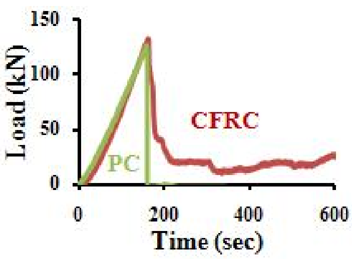

Figure 7: Load-time curves for STS

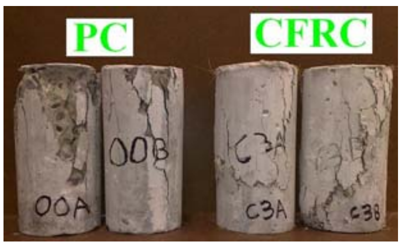

Figure 8: Tested cylinders for MOE

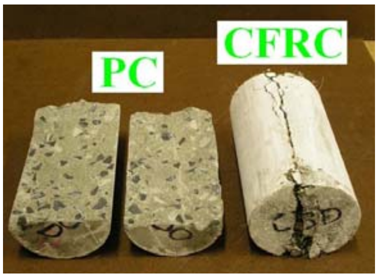

Figure 9: Tested cylinders for STS

(a) Plain concrete **(b) CFRC concrete**

Figure 10: Failure of small beams

Crushed cylinder specimens for MOE and STS are shown in Figures 8 and 9, respectively. The modulus of rupture and corresponding deflection are increased for CFRC specimens as compared to those for plain concrete; but all specimens of PC broke into two pieces (Figure 10a), while CFRC specimens were held together because of the fibres (Figure 10b). A slight decrease in density of CFRC as compared to that of PC is observed as shown in Table 1.

3.2 FORCE DISPLACEMENT CURVES OF LONG BEAMS

Force displacement curves are shown in Figure 11 for both cases of CFRC long beams (without and with rope). The maximum load taken by the CFRC long beam with rope (C3R) is more than that without rope (C3A). Force displacement curves after cracking up to failure in different cycles are also shown in Figure 12 for both cases. In the case of the rope beam, it was possible to go up to five cycles as shown in Figure 12(b), while in the case of the CFRC beam, four cycles were attained.

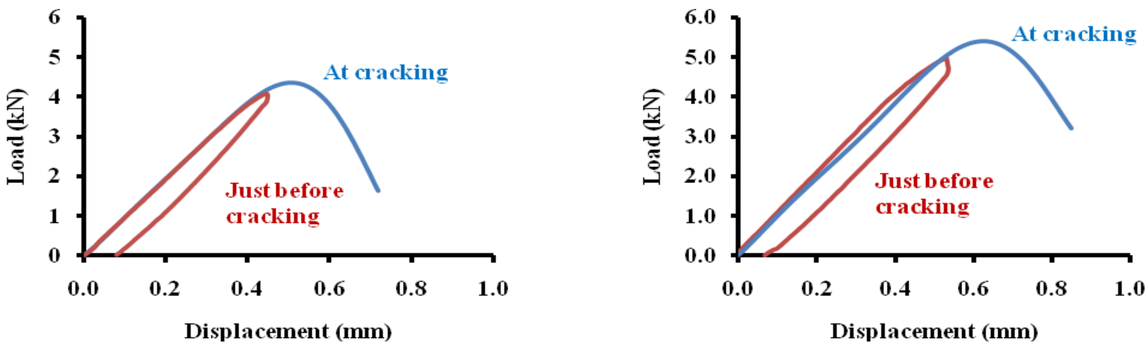

(a) Without rope [C3A] **(b) With rope [C3R]**

Figure 11: Load displacement curves for CFRC beams

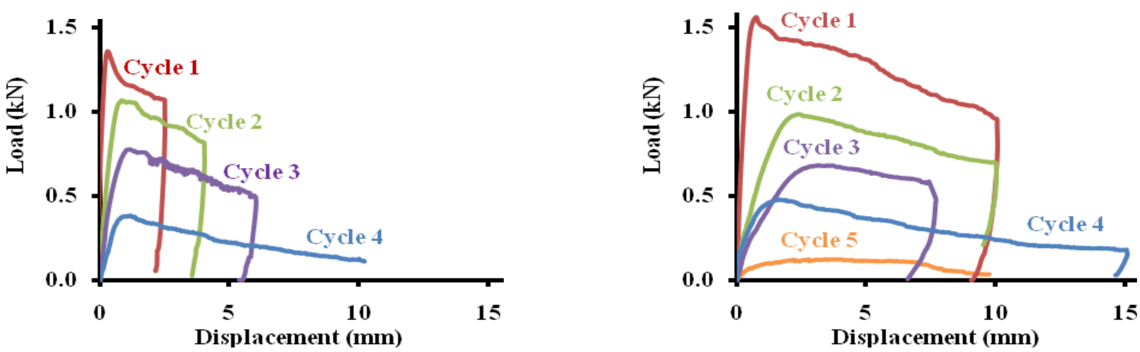

(a) Without rope [C3A] **(b) With rope [C3R]**

Figure 12: Load displacement curves for CFRC beams after cracking up to failure

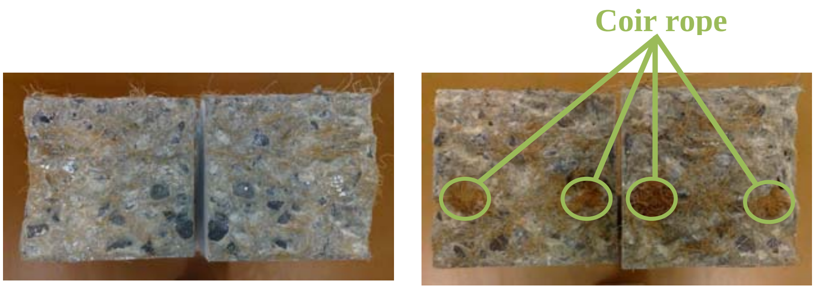

(a) Without rope (C3A) (b) With rope (C3R)

Figure 13: Cracked section of CFRC long beams

Figure 14: Crack profiles

Cracked sections and crack profiles of the CFRC long beams without and with rope are shown in Figures 13 and 14, respectively. It can be observed that the approximately 80% of the fibres are broken and 20% of the fibres are pulled out in the case of the CFRC long beam without rope, while the approximately 60% of the fibres are broken and 40% of the fibres are pulled out in the case of the CFRC long beam with rope.

3.3 DYNAMIC PROPERTIES OF LONG BEAMS

3.3.1 DAMPING

The logarithmic decrement is used for calculating the damping ratio ξ of simply supported CFRC beams without and with rope from the recorded acceleration time histories. Damping ratios ξ, critical damping coefficient c_{cr} and damping coefficient c, are shown in Table 2.

Some selected acceleration time histories are shown in Figures 15 and 16, respectively.

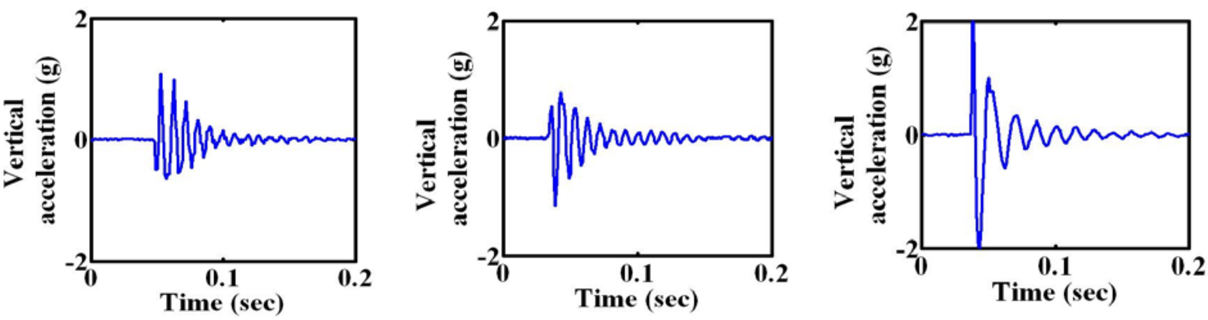

(a) Uncracked beam (b) Cracked beam (c) After crack (cycle 2)

Figure 15: Recorded acceleration time histories of the CFRC beam without rope

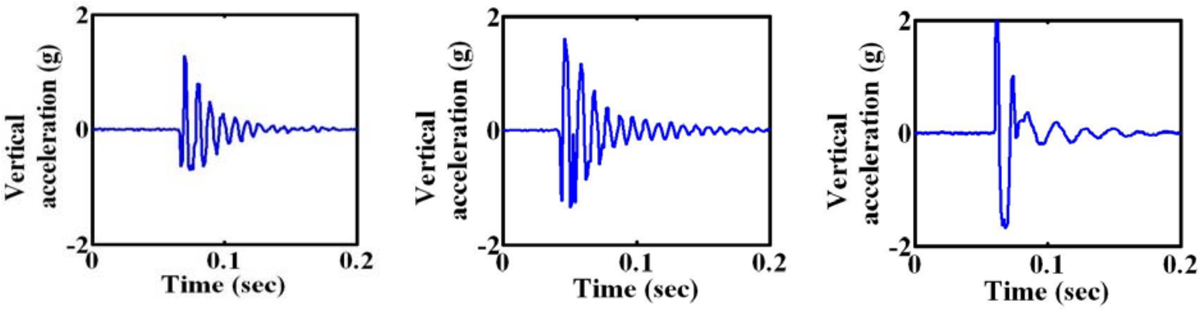

(a) Uncracked beam (b) Cracked beam (c) After crack (cycle 2)

Figure 16: Recorded acceleration time histories of the CFRC beam with rope

Table 2: Dynamic properties of CFRC long beams

Specimen	Label	Condition	Cycle	$P_{Max-static}$ (kN)	Corresponding deflection (mm)	Dynamic properties				
						$P_{(Max-impact)}$ (kN)	ξ (%)	f (Hz)	c_{cr} (kNs/m)	c (kNs/m)
CFRC without rope	C3A	Uncracked beam	-	0	0	0.15	5.24	105.66	29.52	1.55
		Just before crack	-	4.08	0.44	0.14	5.33	104.50	29.19	1.56
		Cracked beam	-	4.21	0.46	0.14	6.18	100.03	27.94	1.72
		After cracks	1	1.36	0.30	0.12	10.03	64.06	17.89	1.79
			2	1.07	0.83	0.19	11.88	55.25	15.43	1.83
			3	0.78	0.16	0.31	16.25	40.97	11.44	1.85
			4	0.38	0.16	0.54	17.22	39.04	11.40	1.96
CFRC with rope	C3R	Uncracked beam	-	0	0	0.16	5.80	105.01	28.45	1.65
		Just before crack	-	5.00	0.54	0.15	6.06	104.62	28.34	1.72
		Cracked beam	-	5.25	0.59	0.19	6.27	100.20	27.15	1.70
		After crack	1	1.56	0.75	0.20	9.51	72.93	19.76	1.88
			2	0.99	2.37	0.24	16.05	45.68	12.38	1.97
			3	0.68	3.18	0.10	10.36	37.47	10.15	1.05
			4	0.48	0.57	0.07	11.93	43.65	11.83	1.45

Note: (1) $P_{Max-static}$ is the applied static load for producing deflection in the beams using the four point load test.
(2) The highlighted properties are obtained from presented acceleration time histories in Figures 15 and 16 for respective tested stage.

3.3.2 NATURAL FREQUENCY

Natural frequency f is calculated from the period of the recorded acceleration (Table 2), and it can be used to define the actual beam Young's modulus at considered damage stages.

4. CONCLUDING REMARKS

Coir fibre reinforced concrete (CFRC) beams with and without rope were tested for their dynamic properties. The workability of CFRC is a major problem because of the presence of fibres. The static properties of CFRC remain, more or less, the same with the note that CFRC beams do not break into two pieces as do beams of normal concrete. Damping of cracked CFRC beams increases as expected, while the natural frequency decreases. It is concluded that CFRC with coir rope rebars has the potential to be used as main structural members due to its increased damping and ductility. However, pouring CFRC into formwork requires special attention, particularly to maintain constant cover for the rope. Bearing capacity of CFRC beams with different rope diameters and the effect of knots at different locations along the length of beams are significant. To clarify these influence factors, further studies are under preparation. CFRC beams with coir rope rebars will be tested under harmonic load using shakers. The effect of earthquake loading on CFRC columns with coir rope as reinforcement will be determined experimentally using the shake table.

ACKNOWLEDGEMENTS

The authors would like to thank all persons who helped them throughout the research, particularly Hou Sou, Anthony Liu, Mark Byrami, Claudio Oyarzo Vera, and the Department of Civil and Environmental Engineering, Golden Bay Cement and Winstone Aggregates for support of this research. The careful review and constructive suggestions by two anonymous reviewers are gratefully acknowledged. The first author also wishes to thank Pakistan Higher Education Commission for supporting his PhD study at the University of Auckland.

REFERENCES

Ghavami, K. (2005). "Bamboo as reinforcement in structural concrete elements." Cement and Concrete Composites, 27(6), 637-649.

Kankam, J. A., Ben-George, M., and Perry, S. H. (1988). "Bamboo-reinforced Concrete beams subjected to third-point loading." ACI Structural Journal, 85(1), 61-67.

Li, Z., Wang, L., and Wang, X. (2007). "Cement composites reinforced with surface modified coir fibers." Journal of Composite Materials, 41(12), 1445-1457.

Sivaraja, M., and Kandasamy, S. (2008). "Characterization of concrete composites for energy absorption." Journal of Reinforced Plastics and Composites, 27(2), 135-144.

Yan, L., Jenkins, C. H., and Pendleton, R. L. (2000). "Polyolefin fiber-reinforced concrete composites. Part I. Damping and frequency characteristics." Cement and Concrete Research, 30(3), 391-401.

Zheng, L., Sharon Huo, X., and Yuan, Y. (2008). "Experimental investigation on dynamic properties of rubberized concrete." Construction and Building Materials, 22(5), 939-947.